JACS
JOURNAL OF THE AMERICAN CHEMICAL SOCIETY

Article

pubs.acs.org/JACS

Attogram Sensing of Trinitrotoluene with a Self-Assembled Molecular Gelator

Kalathil K. Kartha, Sukumaran S. Babu, Sampath Srinivasan, and Ayyappanpillai Ajayaghosh*

Photosciences and Photonics Group, Chemical Sciences and Technology Division, National Institute for Interdisciplinary Science and Technology, CSIR, Trivandrum 695 019, India

Supporting Information

ABSTRACT: Detection of explosives is of utmost importance due to the threat to human security as a result of illegal transport and terrorist activities. Trinitrotoluene (TNT) is a widely used explosive in landmines and military operations that contaminates the environment and groundwater, posing a threat to human health. Achieving the detection of explosives at a sub-femtogram level using a molecular sensor is a challenge. Herein we demonstrate that a fluorescent organogelator exhibits superior detection capability for TNT in the gel form when compared to that in the solution state. The gel when coated on disposable paper strips detects TNT at a record attogram (ag, 10^{-18} g) level (~12 ag/cm^2) with a detection limit of 0.23 ppq. This is a simple and low-cost method for the detection of TNT on surfaces or in aqueous solutions in a contact mode, taking advantage of the unique molecular packing of an organogelator and the associated photophysical properties.

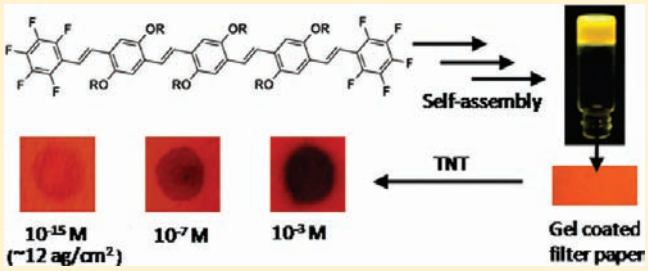

INTRODUCTION

Trinitrotoluene (TNT) is a widely used military explosive, found in different explosive formulations which threaten human life and the environment.[1,2] Therefore, detection of TNT has been a matter of great concern to scientists.[3,4] Even though a large number of reports are available, a simple approach to the detection of explosives at extremely low concentrations still remains a challenge.[5−7] This is particularly true in the case of TNT, due to its relatively low vapor pressure when compared to other explosives.[8] Swager[9] and Trogler[10] independently have made pioneering contributions to the detection of TNT and RDX (Research Department Explosive, chemical name is Cyclotrimethylenetrinitramine). For example, fluorescent polymers containing bulky groups such as pentiptycene moiety, developed by Swager and co-workers, are found to be highly efficient toward the vapor-phase detection of TNT.[9] In an apparently different way, Trogler and co-workers have achieved a sensitivity near the picogram level in solid-phase sensing of explosives using metalloles as the fluorescent donors.[10e] Subsequently, several strategies using quantum dots,[11] gold nanoparticles,[12] silver−gold alloy nanostructures,[13] and molecular imprinting with AuNPs[14] have been reported for the sensing of TNT. Recently, Engel et al. have reported a large array of chemically modified silicon nanowire-based field-effect transistors for the selective detection of TNT with high sensitivity, in which the sensing demands a high-cost instrumental setup.[15]

Self-assembled nanoarchitectures of π-conjugated molecules exhibit properties which are different from those of their individual building blocks.[16] Fluorescence is one such property that shows a significant response to the surrounding medium. For example, fluorescent molecules as a consequence of self-assembly and gelation exhibit significant modulation of the emission color and intensity which is reversible with external inputs.[17] Therefore, fluorescent molecular assemblies and gels are useful candidates for the detection of various analytes.[18,19] In several cases, fluorescent nanofibers obtained by molecular self-assembly have been reported to be good sensing materials for the detection of nitroaromatic explosives due to the unique combination of porous structures with efficient exciton migration in the nanofibers.[18a,b,e] However, detection of explosives at a sub-femtogram level using molecular self-assemblies and gels remains challenging.

We speculated that fluorescent gel fibers exhibiting efficient exciton diffusion and capable of interacting with nitroaromatics may be useful as TNT sensors. With this viewpoint, we have examined several oligo(*p*-phenylenevinylene) (OPV)-based gelators[20] for the detection of TNT. An interesting feature of these gels is their efficient exciton diffusion and energy transfer within the self-assembled aggregates which may be of relevance to the detection of various analytes.[21] However, none of these gelators showed considerable fluorescence quenching with TNT. Therefore, it was obvious that TNT was not able to interact with the gels, probably due to the strong packing of the OPV molecules in the gel form leaving no room for the TNT molecules to be trapped inside. Later we focused our attention on a perfluoroarene-based gelator, **OPVPF**, which forms stable gels in nonpolar solvents at room temperature (critical gelation concentration value in *n*-hexane is 0.75 mM, 1.58 mg/mL),

Received: November 23, 2011
Published: February 17, 2012

with a good solid-state emission quantum yield of 63%.[22] There are several reports on organogels based on arene−perfluoroarene interactions, several formed through a brickwall type of molecular packing.[22−24] We hypothesized that such a brickwall-type molecular packing and the possible charge localization in **OPVPF** (as evident from the electron density distribution calculation using TITAN software, Figure S1) may facilitate strong interaction between electron-deficient aromatic molecules such as TNT. Surprisingly, **OPVPF** gel showed significant quenching of fluorescence in the presence of different nitroaromatic compounds, which led us to a detailed investigation on the potential of the gelator for TNT detection.

RESULTS AND DISCUSSION

In *n*-hexane solution, **OPVPF** exhibits a green fluorescence which upon gelation turns to yellow (Figure 1a,b). The yellow emission could be due to the combination of the green- and red-emitting aggregates present in the gel state. When a hot solution of the gel is dip-coated on a filter paper, the yellow emission further changes to an orange-red emission (Figure 1d). The orange emission of the paper-coated xerogel indicates that the fraction of the green-emitting aggregates has decreased and more of the red-emitting aggregates have formed, giving a combined orange-red emission. The emission color is thermally reversible as observed by the shift in the color from orange-red to green upon heating the filter paper to 70 °C and *vice versa* upon cooling to room temperature. These observations indicate the reversible self-assembly of the gelator molecules to aggregates of different energy levels (Figure 1c,d). The corresponding emission spectra are shown in Figure 1e. Excitation energy diffusion is possible within such aggregates of different energy levels, as evident from the wavelength-dependent lifetime decay profiles (Figure 1f). Scanning electron microscopy (SEM) images of the filter paper before and after coating with the gel are shown in Figure S2. The SEM image of the filter paper before coating with the gel showed the typical micrometer-sized fibers. After coating with the gel, the filter paper fibers were completely covered by the entangled fibers (100−200 nm) of the **OPVPF** molecules (Figure S2). We prepared several samples of **OPVPF** solutions, gels, and the xerogel-coated filter papers to study the response of their fluorescence with different nitroaromatic compounds, and the details are discussed.

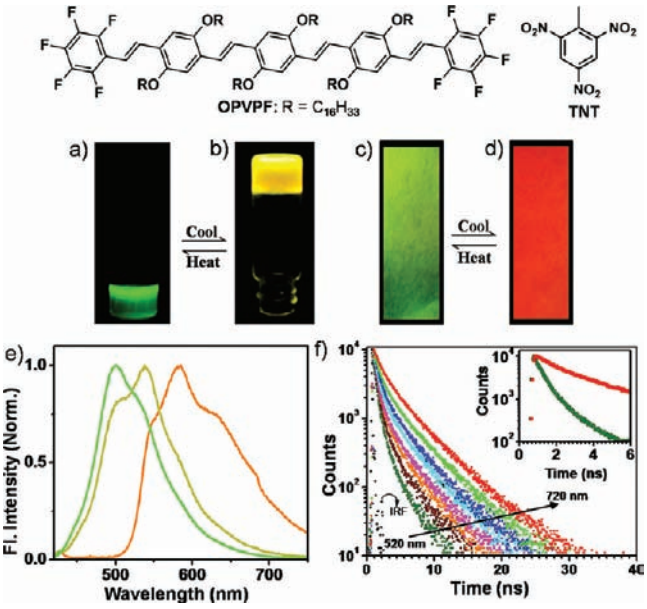

Figure 1. Photographs of (a) *n*-hexane solution and (b) *n*-hexane gel of **OPVPF**. (c,d) Reversible emission color change of filter paper coated with xerogel upon heating to 70 °C and cooling to room temperature. (e) Normalized emission spectra in solution (green line), gel (olive line), and film (orange line) states (λ_{ex} = 400 nm). (f) Wavelength-dependent fluorescence lifetime decay monitored between 520 and 720 nm (λ_{ex} = 440 nm). The inset shows the lifetime decay profiles monitored at 520 nm (green circles) and at 720 nm (red circles), showing a growth corresponding to the excitation of the lower energy aggregates at the initial time scales. IRF = instrument response function.

Our first attempt was to study the fluorescence changes of **OPVPF** in solution upon addition of TNT. The fluorescence response of **OPVPF** (1×10^{-4} M) in chloroform against TNT is shown in Figure 2a as a weak fluorescence quenching. This observation indicates that TNT is not an efficient quencher for **OPVPF** in the isotropic solution state and hence is not suitable for the detection of TNT. Having seen the effect in solution, we decided to test the fluorescence response of the gel state with TNT. A definite amount of *n*-hexane gel (50 μL, 1×10^{-3} M) was dropped on a glass slide (0.5 cm diameter) and dried under vacuum. The xerogel-coated glass slide was placed in a vial containing TNT at room temperature. The emission spectra were measured by using a front-face technique after exposing the film for specific intervals. Surprisingly, significant quenching of the fluorescence was observed (Figure 2b) upon exposure to TNT vapors (as per literature reports, the vapor pressure of TNT at 20 °C is ~10 ng/L or 1 ppb).[15] Nearly 20 ± 5% quenching was noticed within 5 s of exposure (Figure 2b,

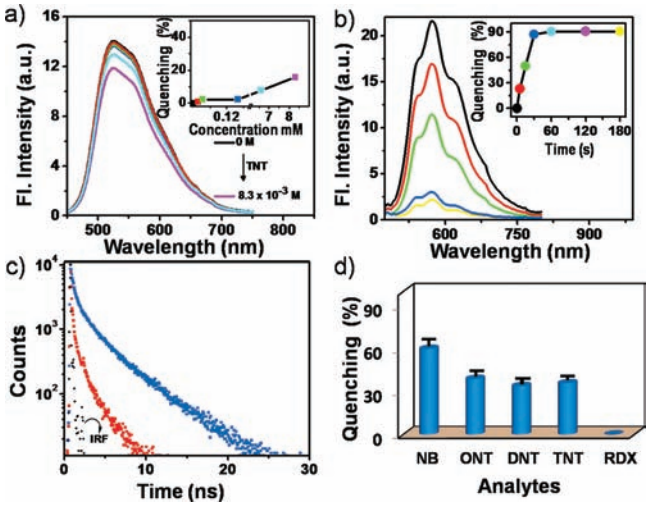

Figure 2. (a) Emission spectra of **OPVPF** in chloroform (1×10^{-4} M) upon addition of different amounts of TNT. Inset: Plot of quenching (%) at 525 nm vs concentration of TNT (λ_{ex} = 400 nm). (b) Time-dependent fluorescence quenching of **OPVPF** xerogel upon TNT vapor exposure. Inset: Plot of fluorescence quenching (%) at 580 nm vs time in seconds. (c) Lifetime decay profiles (λ_{ex} = 440 nm, monitored at 600 nm) of **OPVPF** xerogel before (blue circles) and after (red circles) exposure to TNT vapors for 10 s at room temperature. (d) Comparison of the fluorescence quenching efficiency of **OPVPF** xerogel upon exposure to saturated vapors of different analytes for 10 s in a closed chamber (λ_{ex} = 450 nm; error bar = 5%).

dx.doi.org/10.1021/ja210728c | J. Am. Chem. Soc. 2012, 134, 4834−4841

inset), indicating a fast response time and detection limit between ppb and ppt concentration levels.

In order to understand the excited-state behavior of the **OPVPF** gel, the fluorescence lifetime decay profiles before and after exposure to TNT were recorded. These data of **OPVPF** xerogel (λ_{ex} = 440 nm) exhibited a biexponential character with lifetimes of 1.47 ns (14.4%) and 2.12 ns (85.6%) when monitored at 600 nm. Upon exposure to TNT vapor, a fast biexponential decay with time constants of 0.28 ns (68.3%) and 1.4 ns (31.7%) was observed (Figure 2c). The decrease in the average lifetime can be attributed to the interaction of TNT with the self-assembled xerogel fibrils. A comparison of the response of the gel fibrils against nitrobenzene (NB), *o*-nitrotoluene (ONT), 2,4-dinitrotoluene (DNT), and TNT for a 10 s exposure is shown in Figure 2d. About 90 ± 5% quenching was observed within 40 s of exposure for these different nitroaromatics. In order to test the specificity of the gelator for the detection of nitroaromatics, we have studied the effect of RDX, which is a nonaromatic explosive. Interestingly, the xerogel did not show any fluorescence response when exposed to RDX vapors (Figure 2d).

Confocal laser scanning microscopy (CLSM) images of **OPVPF** gel obtained from *n*-hexane before and after exposure to TNT vapors are shown in Figure 3. After 20 s of exposure to

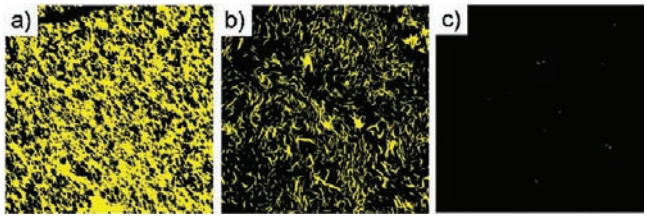

Figure 3. CLSM images of the **OPVPF** gel on glass slides (a) before and (b) 20 and (c) 40 s after exposure to saturated vapors of TNT (~1 ppb) in a closed chamber (λ_{ex} = 438 nm, λ_{em} = 450−550 nm, 10x magnification).

TNT, about 60% of the fluorescence was quenched, and after 40 s, almost complete quenching was observed. These results reveal that **OPVPF** fluorescence is more responsive to the gel phase when compared to the solution state. Since 5% quenching of the fluorescence is sufficient to detect an analyte, the gel is suitable for the sensing of explosives in the native state. The relatively low response of TNT vapors to the gel fluorescence could be attributed to the low equilibrium vapor pressure of TNT (5.6×10^{-6} Torr at 25 °C) when compared to NB (0.15 Torr at 20 °C).[3a] While vapor-phase detection of TNT is extremely important to sense the proximity of explosive devices, a simple method for the on-site instant detection of TNT contamination on surfaces and specimens is equally important. Similar is the case of monitoring for TNT contamination in potable water. Therefore, we decided to test the viability of a contact-mode approach using xerogel-coated disposable paper strips which will be of relevance to the on-site instant detection of TNT.

It is known that explosive particles can contaminate the human body, clothing, and other materials in the surroundings during preparation and packaging of explosive devices or during an explosion.[1c,d] In such cases, contact mode is appropriate to check for residual contamination by an explosive chemical. For this purpose, test strips were prepared by transferring **OPVPF** gel fibers onto a Whatman filter paper by dip-coating a hot solution of the gel, followed by drying under vacuum and cutting the dried filter paper into pieces. The contact-mode response to TNT by the filter paper strips was tested by placing TNT crystals over a test strip for 5 s, resulting in black spots upon illumination with a UV lamp (Figure 4a,c). The same

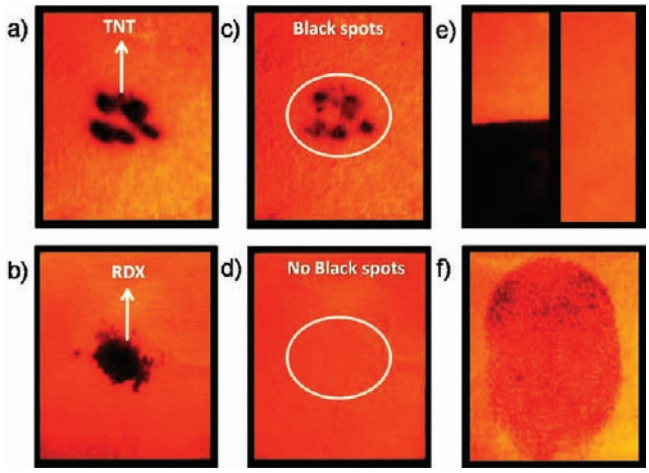

Figure 4. Photographs of **OPVPF**-coated test strips under different experimental conditions. (a) TNT and (b) RDX crystals on top. (c,d) Corresponding photographs upon removal of the crystals after 5 s. (e) After dipping into solutions of TNT (left) and RDX (right) in acetonitrile (1×10^{-3} M). (f) Thumb impression after rubbing with TNT crystals. All photographs were taken under 365 nm UV illumination.

experiment was repeated with RDX, and no spots corresponding to fluorescence quenching were found (Figure 4b,d). In addition, the test strips were dipped into acetonitrile solutions of TNT and RDX, and fluorescence quenching was observed only in the case of TNT (Figure 4e). In another experiment, a human thumb was rubbed with TNT (***caution***: no direct contact, use a glove!), and then all visible TNT particles were brushed off, followed by pressing the thumb against a test strip. The fingerprint of the thumb could be seen as quenched luminescence when illuminated with UV light (Figure 4f). As a control experiment, the thumb (gloved) which was not contaminated with TNT was pressed on the test strip, and no fingerprint was seen. These images illustrate the utility of the gel-coated test strips for the on-site instant visualization of trace residues of TNT present on a specimen.

Detection of extremely small amounts of TNT on different substrates or from debris of explosions could be better performed by extraction with a suitable solvent and then dilution to a required volume followed by spot-testing using the paper strips. To test this possibility, aqueous solutions of different analytes (acetonitrile:water, 0.5:9.5 v/v) were prepared, and 10 μL of each solution was placed on the paper test strips to give a spot area of ~0.2 cm^2 (aqueous condition was preferred to avoid any possible leaching of the gelator from the test strip). The visual fluorescence response of different nitroaromatics at different concentrations by contact-mode detection on filter paper test strips is shown in Figure 5a. The minimum amount of TNT detectable by the naked eye was as low as 10 μL of 1×10^{-15} M solution, thereby registering a detection limit of 0.227 parts per quadrillion (ppq). The fluorescence spectral changes of the test strips on contact with TNT for a wide range of concentration is shown in Figure 5b, and the corresponding fluorescence quenching

dx.doi.org/10.1021/ja210728c | *J. Am. Chem. Soc.* 2012, 134, 4834−4841

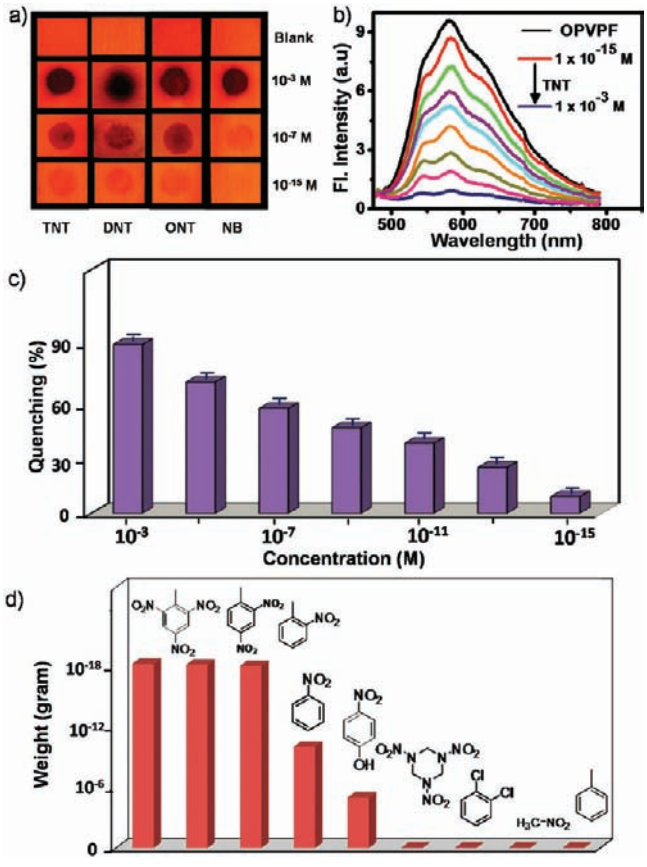

Figure 5. (a) Photograph of the fluorescence quenching of **OPVPF**-coated test strips by nitroaromatics on contact mode (10 μL of the analyte with a spot area of ~0.2 cm^2) when viewed under 365 nm UV illumination. (b) Emission spectral change (λ_{ex} = 450 nm) of the test strips against concentration of added TNT (10 μL, 1 × 10^{-15}–1 × 10^{-3} M). (c) Plot of the emission at 580 nm (%) of the test strips against concentration of added TNT in acetonitrile:water (0.5:9.5, 10 μL, 1 × 10^{-15}–1 × 10^{-3} M). (d) Contact-mode detection of the lowest amount of different analytes by the emission quenching of the test strip. In all experiments, a front-face technique was used to record the emission from the test strips.

(%) at 580 nm is shown in Figure 5c. A comparison of the minimum detectable amounts of the analytes estimated from the fluorescence quenching indicates that nonaromatic explosives and aromatic compounds without nitro groups are not sensed by the test strips (Figure 5d). Fluorescence quenching could be visually detected to the level of 1.37 × 10^{-18} g (ONT), 1.82 × 10^{-18} g (DNT), 2.27 × 10^{-18} g (TNT), and 1.23 × 10^{-10} g (NB) using the test strips when 10 μL of the analyte was spotted with a spread of ~0.2 cm^2. From these data, the detection limit of TNT is calculated as ~12 ag/cm^2, which is much lower than the values previously achieved using a surface detection method (Table S1).[10e,11b] Thus, in the cases of TNT, DNT, and ONT, the limit of detection up to a record attogram level with sensitivity in the range of ppq could be achieved.

Nitroaromatic compounds are environmental contaminants that pollute soil and groundwater after military operations.[10d] The amount of TNT above 2 ppb in drinking water can be toxic and carcinogenic.[1c,d] The intake of TNT may cause liver damage, gastritis, aplastic anemia, cyanosis, and dermatitis.[25] Hence, the detection of nitroaromatics, particularly TNT, in potable water for low-level contamination is of great relevance.[10d,26] With this objective, aqueous solutions of TNT were prepared, and 10 μL aliquots of each of these solutions were placed on the paper test strips, covering an area of ~0.2 cm^2. The fluorescence spectral change upon addition of the test samples is shown in Figure 6a, and the corresponding

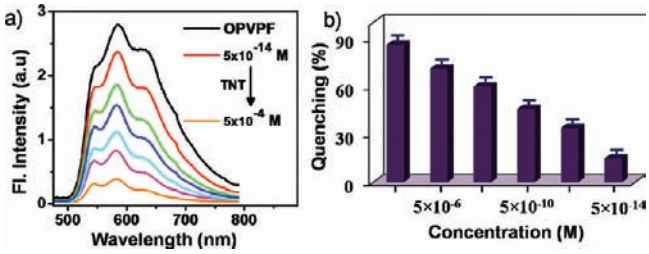

Figure 6. (a) Emission spectral change (λ_{ex} = 450 nm) of the **OPVPF**-coated test strips with added amount of TNT in potable water (10 μL, 5 × 10^{-14}–5 × 10^{-4} M). (b) Corresponding % quenching of fluorescence at 580 nm.

quenching (%) bar diagram is shown in Figure 6b. The lowest amount of TNT in potable water detectable by the naked eye on filter paper strips is 5 × 10^{-14}–1 × 10^{-15} M, which corresponds to a sensitivity in the range of 11.4–0.23 ppq.

To get insight on the mode of interaction and molecular packing, X-ray diffraction (XRD) analysis of **OPVPF** gel before and after exposure to TNT was performed (Figure 7). The XRD pattern before exposure to TNT (Figure 7a) indicates a brickwall-type arrangement of the molecules, which is in analogy to the previous reports.[22,23] For example, the crystal XRD data of a bis(pentafluorostyryl)stilbene derivative showed a brickwall-type assembly in which each brick is situated over the gap between the bricks in the row below.[23a] In a similar situation, each of the terminal fluorinated aromatic rings of **OPVPF** is sandwiched between the central aromatic rings of the neighboring **OPVPF** molecules, and vice versa. Thus, in addition to the face-to-face π-stacking, the molecules are involved in C–F···H–C interactions (Figure S3). The peak corresponding to a *d*-spacing of 3.74 Å could be the π-stacking distance between two **OPVPF** molecules. The *d*-spacing of 7.13 Å corresponds to the distance between the alternate (top and bottom) **OPVPF**. The diffraction peak corresponding to 5.97 Å could be the end-to-end distance between two **OPVPF** molecules. The *d*-spacings of ~9.0 and ~4.4 Å may correspond to the packing distances of the alkyl side chains in the brickwall-type assembly. The xerogel-coated glass plate after exposure to saturated TNT vapors exhibited almost identical XRD patterns (Figure 7b). A similar experiment was conducted with dried xerogel after dipping in TNT solution in water (5 × 10^{-14} M) (Figure 7c). In this case also, only negligible changes were observed in the diffraction peaks, indicating that the **OPVPF** packing is not considerably disturbed either by TNT vapors or by the solvent. This is further confirmed by the film-state absorption and reflection spectra of the gelator before and after contact with TNT solutions (Figure S4), which did not show any visible change. This observation also indicates that there is no ground-state charge transfer between **OPVPF** and TNT. Therefore, we conclude that the TNT molecules are trapped inside the interstitial space of the **OPVPF** molecules without changing the overall brickwall-type molecular packing, and the observed fluorescence quenching is due to excited-state processes.

dx.doi.org/10.1021/ja210728c | J. Am. Chem. Soc. 2012, 134, 4834–4841

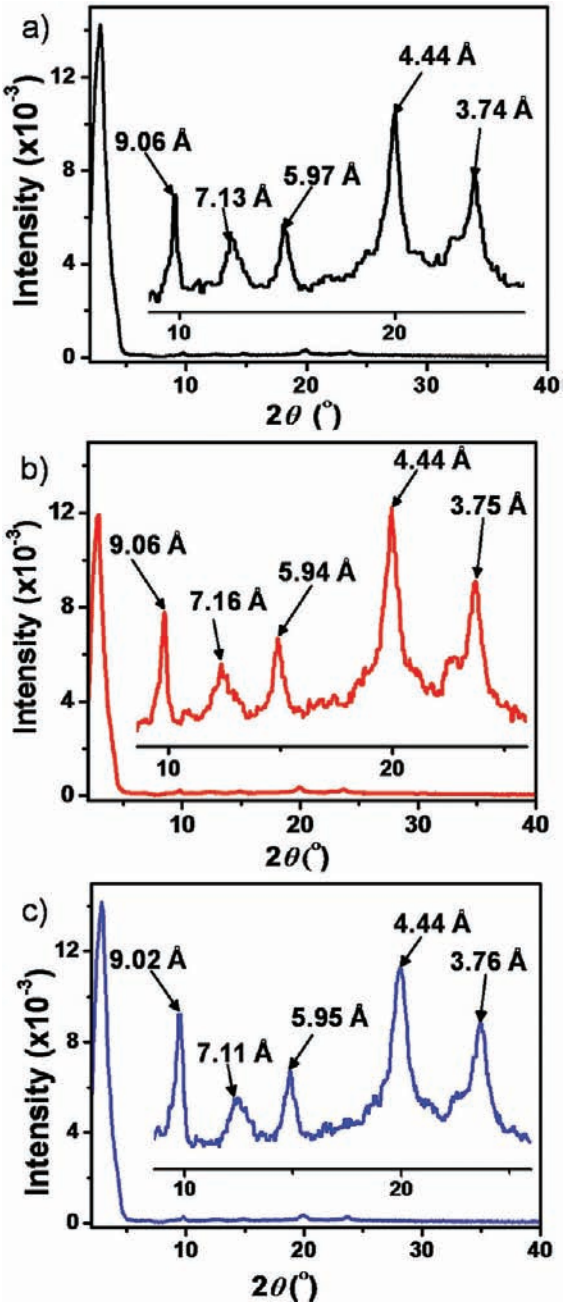

Figure 7. XRD patterns of the xerogel of **OPVPF** (a) before, (b) after TNT vapor exposure, and (c) after TNT contact-mode exposure in water. Insets show the 2θ values of the zoomed region between 8.6 and 26°.

Based on the above observations, a plausible mechanism of the fluorescence quenching with TNT in the xerogel state is depicted in Figure 8. The gel fiber bundles of **OPVPF** are comprised of nanosized fibrils, which in turn are formed by self-assembled aggregates having different energy levels. Each aggregate is formed by the brickwall-type arrangement of **OPVPF** with interstitial free space within the aggregates with a vertical distance of ~7.13 Å and a horizontal distance of 5.97 Å, as shown in Figure 8. Since the calculated maximum molecular length of TNT (between the methyl group and the oppositely placed nitro group) is ~6.86 Å (Figure S1), it can fit vertically into the free space through electrostatic interaction with **OPVPF** (Figure 8). Thus, the possible edge-to-face π-stacking

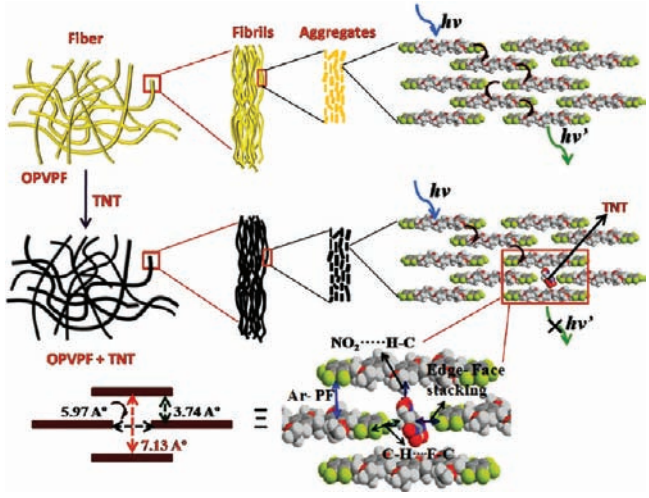

Figure 8. Schematic illustration of the fluorescence quenching mechanism of **OPVPF** xerogel fibers in the presence of attogram levels of TNT. The bottom right picture shows various noncovalent interactions, and the bottom left picture shows the approximate distance between neighboring **OPVPF** in a brickwall-type arrangement.

between the electron-deficient aromatic core of TNT and the electron-rich perfluoroarene moieties of **OPVPF** favors the formation of a tight complex. Such an interaction may be further assisted by the hydrogen bonding between the nitro groups in TNT and the hydrogen atoms in the **OPVPF** backbone. Similarly, hydrogen bonding is also possible between the hydrogen atoms in the methyl group of TNT and the fluorine atoms of the **OPVPF**. Due to the cooperative interaction of the above weak forces, whenever the xerogel fibers are in contact with a TNT molecule, it gets entrapped and acts as a fluorescence trap. In addition, there is the possibility of the TNT molecules getting trapped between the interstitial sites of the elementary fibrils of the xerogel due to the exposed pentafluoro aryl moieties.

The efficient fluorescence quenching of **OPVPF** xerogel-coated filter paper by an extremely small amount of TNT could be explained by a faster exciton diffusion mechanism, as described earlier by Swager and co-workers as in the case of conjugated polymers.[9b,27] Time-resolved emission studies (TRES) of the xerogel indicated a dynamic red shift of the emission spectra from 540 to 580 nm when collected after 56 ps and 1.3 ns, respectively. This observation reveals the possibility of fast excitation energy migration in the self-assembly (Figure S5).[22] The possibility of energy migration is further supported by the wavelength-dependent fluorescence decay profiles, as shown in Figure 1f. At lower wavelength (520 nm) the decay was fast, whereas at higher wavelength (720 nm) the decay was relatively slow, with a growth component at the lower time scales (0.11 and 0.5 ns, respectively), indicating the singlet excitation of the lower energy aggregates by the initially excited higher energy aggregates (Figure 1f, inset). These data indicate that the self-assembled gelator favors exciton hoping via intermolecular electronic coupling, thereby facilitating long-range exciton diffusion in the xerogel state. Thus, the fast excitation energy diffusion within the fibrils and between the fibrils facilitates efficient fluorescence quenching by possible energy-transfer and electron-transfer mechanisms, even with extremely low quantities of the quencher, resulting in attogram level detection.

dx.doi.org/10.1021/ja210728c | J. Am. Chem. Soc. 2012, 134, 4834–4841

In the case of Föster-type energy transfer, a single quencher molecule can cover approximately a distance of 1−10 nm. However, in the case of **OPVPF** xerogel fibers, due to efficient excitation energy migration, a single quencher molecule in principle may cover a longer distance than the normal Föster distance, making the quenching more efficient. Thus, when a 10 μL volume of 1×10^{-15} M TNT solution is spotted on the filter paper test trip covering an area of ~0.2 cm^2, 2.27 ag of the TNT present can get entrapped at different locations, which will be sufficient to have a detectable fluorescence quenching of the spotted area, giving a detection limit of ~12 ag/cm^2. In the solution, since the gelator molecules are in the isotropic state, such a mechanism is not feasible, and hence the sensitivity is extremely low for TNT, as observed. The weak fluorescence quenching with nonaromatic and poorly electron-deficient aromatic compounds indicates that the binding strength of the analyte with the gelator is crucial for the low-level detection.

■ CONCLUSIONS

In conclusion, the attogram level detection of TNT using a self-assembled fluorescent gelator has been demonstrated. The gelator molecule (**OPVPF**) is not efficient for the sensing of TNT in the solution state, whereas in the xerogel state high sensitivity has been achieved. This finding highlights the unique capability of the self-assembled fibrous structures as new materials over the individual molecules for a specific application. While the sensitivity to TNT in the vapor phase was in the ppt range, the detection level was in the ppq range in the contact mode. The attogram detection level with high sensitivity achieved using disposable filter paper-based test strips allows a simple and low-cost protocol for the on-site instant detection of TNT on contaminated specimens, as well as monitoring of TNT contamination in groundwater, which has great relevance to human health and safety.

■ EXPERIMENTAL SECTION

General Procedures. Unless otherwise stated, all materials and reagents were purchased from commercial suppliers. The solvents and reagents were purified and dried by standard methods prior to use. **OPVPF** was synthesized as per our previous report.[22] TNT and RDX were obtained from High Energy Materials Research Laboratory, Pune, and recrystallized from ethanol.

Spectral Measurements. The absorption or reflection spectra were recorded on a Shimadzu UV−vis recording spectrophotometer UV-2100 with $BaSO_4$ as standard. The emission spectra were recorded on a SPEX-Flourolog F112X spectrofluorimeter using a front face sample holder.

Lifetime Measurements. Fluorescence lifetimes were measured using IBH (FluoroCube) time-correlated picosecond single photon counting (TCSPC) system. Solutions were excited with a pulsed diode laser (<100 ps pulse duration) at a wavelength of 440 nm (NanoLED-10) with a repetition rate of 1 MHz. The detection system consists of a microchannel plate photomultiplier (5000U-09B, Hamamatsu) with a 38.6 ps response time coupled to a monochromator (5000M) and TCSPC electronics (DataStation Hub including Hub-NL, NanoLED controller and preinstalled Fluorescence Measurement and Analysis Studio (FMAS) software). The fluorescence lifetime values were determined by deconvoluting the instrument response function with biexponential decay using DAS6 decay analysis software. The quality of the fit has been judged by the fitting parameters such as χ^2 (<1.2) as well as the visual inspection of the residuals. All measurements were carried out using a front face sample holder (5000U-04).

Flourescence Quantum Yield Measurements. Fluorescence quantum yield of the gel-coated filter paper was measured using a calibrated integrating sphere in a SPEX Fluorolog spectrofluorimeter. A Xe-arc lamp was used to excite the sample placed in the sphere, with 450 nm as the excitation wavelength. Absolute fluorescence quantum yield was calculated on the basis of the de Mello method[28] using the equation

$$\phi_{PL} = [E_i(\lambda) - (1 - A)E_0(\lambda)]/L_e(\lambda)A \quad (1)$$

In eq 2

$$A = [L_0(\lambda) - L_i(\lambda)]/L_0(\lambda) \quad (2)$$

where $E_i(\lambda)$ and $E_0(\lambda)$ are respectively the integrated luminescence as a result of direct excitation of sample and secondary excitation. A is the absorbance of the sample calculated using eq 1. $L_i(\lambda)$ is the integrated excitation when the sample is directly excited, $L_0(\lambda)$ is the integrated excitation when the excitation light first hits the sphere and reflects to the sample, and $L_e(\lambda)$ is the integrated excitation profile for an empty sphere.

Scanning Electron Microscopy. SEM images were taken on a JEOL 5600 LV scanning electron microscope with an accelerating voltage of 12−15 kV after sputtering with gold.

Confocal Laser Scanning Microscopy. CLSM images were recorded on a Leica-DMIR2 Optical Microscope using UV light (438 nm) as the excitation source, and the emission was collected between 450 to 550 nm with 10x magnification. Samples were prepared by drop-casting *n*-hexane solution on a glass slide followed by slow evaporation.

X-ray Diffraction. *n*-Hexane gel of **OPVPF** (5 mg/mL) was transferred to a glass plate, and the prepared film was kept a day for slow evaporation of the solvent and finally dried under vacuum. The same xerogel-coated glass plate was exposed to saturated TNT vapor in a clossed vessel for 5 min, and immediately after exposure the difraction pattern was recorded. A similar experiment was conducted with the dried xerogel after dipping in TNT solution in water (5×10^{-14} M). The X-ray diffractograms of the samples before and after exposure to TNT were recorded on a Phillips diffractometer using Ni-filtered Cu Kα radiation.

Preparation of Filter Paper Test Strips. Filter paper (5 cm × 2 cm) test strips were prepared by coating the melted **OPVPF** *n*-hexane gel (1×10^{-3} M) followed by removal of solvent under vacuum at room temperature. The dip-coating of the hot solution above CGC allowed the spontaneous self-assembly of the gelator on the filter paper. The gel-coated filter papers were then cut into 10 pieces (1 cm × 1 cm) to get the test strips and used for the detection of explosives.

Contact Mode Visual Detection of TNT. Aqueous samples were prepared by dissolving TNT in acetonitrile:water (0.5:9.5) mixture. The explosive solutions were spotted onto the test strips at the desired concentration level using a glass microsyringe. A solvent blank was spotted near to the spot of each explosive. In order to ensure consistent analysis, all depositions were prepared from a 10 μL volume, thereby producing a spot of ~0.5 cm in diameter. After solvent evaporation, the filter paper was illuminated with 365 nm UV light. The dark spots were identified by an independent observer, and each set of experiments was repeated three times for consistency. The detection limits were calculated from the

lowest concentration of the explosive that enabled an independent observer to detect the quenching visually.

Quantitative Detection of TNT by Emission Quenching. The required analyte solutions of various concentrations (1×10^{-15}–1×10^{-3} M) were added to each strip, and the solvents were allowed to evaporate. The film was placed in such a way that the excitation beam falls on the spot where TNT is added. Emission was collected by a front face technique using a film sample holder. Emission of a blank sample was monitored by the addition of solvent alone.

Detection of TNT in Potable Water. A stock solution (5×10^{-4} M) was prepared by dissolving TNT in potable water by overnight stirring at room temperature (0.114 mg/mL). This solution was diluted to different concentrations and used as the test samples. The test samples (10 μL) were spoted to the test strips, and the fluorescence quenching was monitored under 365 nm illumination by an independent observer. The minimum detection level of TNT was qualitatively judged by the naked eye detectable fluorescence quenching on the test strip and quantitatively determined by measuring the fluorescence quenching (%) using the front face technique.

■ ASSOCIATED CONTENT

Ⓢ Supporting Information

SEM images, proposed molecular packing of **OPVPF** in the xerogel state, absorption and reflection spectra of **OPVPF** xerogel, energy-minimized structures of **OPVPF**, time-resolved emission study of **OPVPF** xerogel, and a comparative chart of the limit of detection. This material is available free of charge via the Internet at http://pubs.acs.org.

■ AUTHOR INFORMATION

Corresponding Author

ajayaghosh62@gmail.com

Notes

The authors declare no competing financial interest.

■ ACKNOWLEDGMENTS

We thank CSIR, Government of India, New Delhi, for financial support under NWP-023, DST and JSPS for an exchange project, and Department of Atomic Energy, Government of India, for a DAE-SRC Outstanding Researcher Award to A.A. (Manuscript no. PPG-324 from NIIST). K.K.K. is grateful to CSIR for a fellowship. We acknowledge Mr. P. Gurusamy and Mr. P. Chandran of NIIST for XRD and SEM, respectively, and Dr. R. V. Omkumar of the Rajiv Gandhi Centre for Biotechnology (RGCB) for confocal laser scanning microscopy. We thank HEMRL, Pune for samples of TNT and RDX.

■ REFERENCES

(1) (a) Fainberg, A. *Science* **1992**, *255*, 1531. (b) Yinon, J. *Forensic and Environmental Detection of Explosives*; John Wiley & Sons Ltd.: Chichester, 1999. (c) Albert, K. J.; Lewis, N. S.; Schauer, C. L.; Sotzing, G. A.; Stitzel, S. E.; Vaid, T. P.; Walt, D. R. *Chem. Rev.* **2000**, *100*, 2595. (d) Kim, T. H.; Lee, B. Y.; Jaworski, J.; Yokoyama, K.; Chung, W.-J.; Wang, E.; Hong, S.; Majumdar, A.; Lee, S.-W. *ACS nano* **2011**, *5*, 2824.

(2) (a) Pinnaduwage, L. A.; Gehl, A.; Hedden, D. L.; Muralidharan, G.; Thundat, T.; Lareau, R. T.; Sulchek, T.; Manning, L.; Rogers, B.; Jones, M.; Adams, J. D. *Nature* **2003**, *425*, 474. (b) Moore, D. S. *Rev. Sci. Instrum.* **2004**, *75*, 2499. (c) Tenhaeff, W. E.; McIntosh, L. D.; Gleason, K. K. *Adv. Funct. Mater.* **2010**, *20*, 1144.

(3) (a) Yinon, J. *Forensic and Environmental Detection of Explosives*; John Wiley & Sons: Chichester, 1999. (b) Trogler, W. C. In *NATO ASI Workshop, Electronic Noses & Sensors for the Detection of Explosives*; Gardner, J. W., Yinon, J., Eds.; Kluwer Academic Publishers: Netherlands, 2004.

(4) (a) Czarnik, A. W. *Nature* **1998**, *394*, 417. (b) Oxley, J. C.; Smith, J. L.; Resende, E.; Pearce, E.; Chamberlain, T. *J. Forensic Sci.* **2003**, *48*, 1. (c) Singh, S. *J. Hazard. Mater.* **2007**, *144*, 15.

(5) (a) Germain, M. E.; Knapp, M. J. *Chem. Soc. Rev.* **2009**, *38*, 2543. (b) Salinas, Y.; Martınez-Manez, R.; Marcos, M. D.; Sancenon, F.; Costero, A. M.; Parra, M.; Gil, S. *Chem. Soc. Rev.* **2012**, *41*, 1261.

(6) Goldman, E. R.; Medintz, I. L.; Whitley, J. L.; Hayhurst, A.; Clapp, A. R.; Uyeda, H. T.; Deschamps, J. R.; Lassman, M. E.; Mattoussi, H. *J. Am. Chem. Soc.* **2005**, *127*, 6744.

(7) (a) Lan, A.; Li, K.; Wu, H.; Olson, D. H.; Emge, T. J.; Ki, W.; Hong, M.; Li, J. *Angew. Chem., Int. Ed.* **2009**, *48*, 2334. (b) Pramanik, S.; Zheng, C.; Zhang, X.; Emge, T. J.; Li, J. *J. Am. Chem. Soc.* **2011**, *133*, 4153.

(8) (a) Howard, P. H., Meylan, W. M., Eds. *Handbook of Physical Properties of Organic Chemicals*; CRC Press: Boca Raton, FL, 1997. (b) Pushkarsky, M. B.; Dunayevskiy, I. G.; Prasanna, M.; Tsekoun, A. G.; Go, R.; Kumar, C.; Patel, N. *Proc. Natl. Acad. Sci. U.S.A.* **2006**, *103*, 19630.

(9) (a) Yang, J.-S.; Swager, T. M. *J. Am. Chem. Soc.* **1998**, *120*, 11864. (b) Yang, J.-S.; Swager, T. M. *J. Am. Chem. Soc.* **1998**, *120*, 5321. (c) McQuade, D. T.; Pullen, A. E.; Swager, T. M. *Chem. Rev.* **2000**, *100*, 2537. (d) Swager, T. M.; Wosnick, J. H. *MRS Bull.* **2002**, *27*, 446. (e) Zahn, S.; Swager, T. M. *Angew. Chem., Int. Ed.* **2002**, *41*, 4225. (f) Rose, A.; Zhu, Z.; Madigan, C. F.; Swager, T. M.; Bulovi, V. *Nature* **2005**, *434*, 876. (g) Thomas, S. W.; Joly, G. D.; Swager, T. M. *Chem. Rev.* **2007**, *107*, 1339. (h) Swager, T. M. *Acc. Chem. Res.* **2008**, *41*, 1181.

(10) (a) Sohn, H.; Calhoun, R. M.; Sailor, M. J.; Trogler, W. C. *Angew. Chem., Int. Ed.* **2001**, *40*, 2104. (b) Sohn, H.; Sailor, M. J.; Magde, D.; Trogler, W. C. *J. Am. Chem. Soc.* **2003**, *125*, 3821. (c) Toal, S. J.; Magde, D.; Trogler, W. C. *Chem. Commun.* **2005**, 5465. (d) Sanchez, J. C.; DiPasquale, A. G.; Rheingold, A. L.; Trogler, W. C. *Chem. Mater.* **2007**, *19*, 6459. (e) Sanchez, J. C.; Trogler, W. C. *J. Mater. Chem.* **2008**, *18*, 3143.

(11) (a) Goldman, E. R.; Medintz, I. L.; Whitley, J. L.; Hayhurst, A.; Clapp, A. R.; Uyeda, H. T.; Deschamps, J. R.; Lassman, M. E.; Mattoussi, H. *J. Am. Chem. Soc.* **2005**, *127*, 6744. (b) Zhang, K.; Zhou, H.; Mei, Q.; Wang, S.; Guan, G.; Liu, R.; Zhang, J.; Zhang, Z. *J. Am. Chem. Soc.* **2011**, *133*, 8424.

(12) Qu, W. G.; Deng, B.; Zhong, S. L.; Shi, H. Y.; Wang, S. S.; Xu, A. W. *Chem. Commun.* **2011**, *47*, 1237.

(13) Yang, L. B.; Chen, G. Y.; Wang, J.; Wang, T. T.; Li, M. Q.; Liu, J. H. *J. Mater. Chem.* **2009**, *19*, 6849.

(14) (a) Riskin, M.; Vered, R. T.; Bourenko, T.; Granot, E.; Willner, I. *J. Am. Chem. Soc.* **2008**, *130*, 9726. (b) Riskin, M.; Tel-Vered, R.; Lioubashevski, O.; Willner, I. *J. Am. Chem. Soc.* **2009**, *131*, 7368. (c) Frasconi, M.; Tel-Vered, R.; Riskin, M.; Willner, I. *J. Am. Chem. Soc.* **2010**, *132*, 9373.

(15) Engel, Y.; Elnathan, R.; Pevzner, A.; Davidi, G.; Flaxer, E.; Patolsky, F. *Angew. Chem., Int. Ed.* **2010**, *49*, 6830.

(16) (a) Ajayaghosh, A.; Praveen, V. K. *Acc. Chem. Res.* **2007**, *40*, 644. (b) Ajayaghosh, A.; Praveen, V. K.; Vijayakumar, C. *Chem. Soc. Rev.* **2008**, *37*, 109. (c) Ariga, K.; Hill, J. P.; Lee, M. V.; Vinu, A.; Charvet, R.; Acharya, S. *Sci. Technol. Adv. Mater.* **2008**, *9*, 014109. (d) Cardolaccia, T.; Li, Y.; Schanze, K. S. *J. Am. Chem. Soc.* **2008**, *130*, 2535. (e) Babu, S. S.; Kartha, K. K.; Ajayaghosh, A. *J. Phys. Chem. Lett.* **2010**, *1*, 3413. (f) Kim, H.; Kim, T.; Lee, M. *Acc. Chem. Res.* **2011**, *44*, 72.

(17) (a) Ajayaghosh, A.; Vijayakumar, C.; Praveen, V. K.; Babu, S. S.; Varghese, R. *J. Am. Chem. Soc.* **2006**, *128*, 7174. (b) Ajayaghosh, A.; Praveen, V. K.; Vijayakumar, C.; George, S. J. *Angew. Chem., Int. Ed.* **2007**, *46*, 6260. (c) Ajayaghosh, A.; Praveen, V. K.; Srinivasan, S.; Varghese, R. *Adv. Mater.* **2007**, *19*, 411. (d) Vijayakumar, C.; Praveen, V. K.; Ajayaghosh, A. *Adv. Mater.* **2009**, *21*, 2059. (e) Srinivasan, S.;

Babu, P. A.; Mahesh, S.; Ajayaghosh, A. *J. Am. Chem. Soc.* **2009**, *131*, 15122.
(18) (a) Naddo, T.; Che, Y.; Zang, W.; Balakrishnan, K.; Yang, X.; Yen, M.; Zhao, J.; Moore, J. S.; Zhang, L. *J. Am. Chem. Soc.* **2007**, *129*, 6978. (b) Zang, L.; Che, Y.; Moore, J. S. *Acc. Chem. Res.* **2008**, *41*, 1596. (c) Zyryanov, G. V.; Palacios, M. A.; Anzenbacher, P. *Org. Lett.* **2008**, *10*, 3681. (d) Vijayakumar, C.; Tobin, G.; Schmitt, W.; Kima, M. -J.; Takeuchi, M. *Chem. Commun.* **2010**, *46*, 874. (e) Zhang, C.; Che, Y.; Yang, X.; Bunes, B. R.; Zang, L. *Chem. Commun.* **2010**, *46*, 5560. (f) Giansante, C.; Olive, A. G. L.; Schäfer, C.; Raffy, G.; Del Guerzo, A. *Anal. Bioanal. Chem.* **2010**, *396*, 125. (g) Gole, B.; Shanmugaraju, S.; Bar, A. K.; Mukherjee, P. S. *Chem. Commun.* **2011**, *47*, 10046. (h) Bhalla, V.; Singh, H.; Kumar, M.; Prasad, S. K. *Langmuir* **2011**, *27*, 15275.
(19) (a) An, B.; Kwon, S.; Jung, S.; Park, S. Y. *J. Am. Chem. Soc.* **2002**, *124*, 14410. (b) An, B.; Kwon, S.; Park, S. Y. *Bull. Kor. Chem. Soc.* **2005**, *26*, 1555. (c) Lee, H.; Jung, S. H.; Han, W. S.; Moon, J. H.; Kang, S.; Lee, J. Y.; Jung, J. H.; Shinkai, S. *Chem.—Eur. J.* **2011**, *17*, 2823. (d) Cox, J. R.; Muller, P.; Swager, T. M. *J. Am. Chem. Soc.* **2011**, *133*, 12910.
(20) (a) Ajayaghosh, A.; George, S. J. *J. Am. Chem. Soc.* **2001**, *123*, 5148. (b) George, S. J.; Ajayaghosh, A. *Chem.—Eur. J.* **2005**, *11*, 3217. (c) Babu, S. S.; Mahesh, S.; Kartha, K. K.; Ajayaghosh, A. *Chem.—Asian J.* **2009**, *4*, 824.
(21) (a) Ajayaghosh, A.; George, S. J.; Praveen, V. K. *Angew. Chem., Int. Ed.* **2003**, *42*, 332. (b) Praveen, V. K.; George, S. J.; Varghese, R.; Vijayakumar, C.; Ajayaghosh, A. *J. Am. Chem. Soc.* **2006**, *128*, 7542. (c) Vijayakumar, C.; Praveen, V. K.; Kartha, K. K.; Ajayaghosh, A. *Phys. Chem. Chem. Phys.* **2011**, *13*, 4942.
(22) Babu, S. S.; Praveen, V. K.; Prasanthkumar, S.; Ajayaghosh, A. *Chem.—Eur. J.* **2008**, *14*, 9577.
(23) (a) Feast, W. J.; Lçvenich, P. W.; Puschmann, H.; Taliani, C. *Chem. Commun.* **2001**, 505. (b) Capelli, R.; Loi, M. A.; Taliani, C.; Hansen, H. B.; Murgia, M.; Ruani, G.; Muccini, M.; Lovenich, P. W.; Feast, W. J. *Synth. Met.* **2003**, *139*, 909.
(24) For arene—perfluoroarene-based gelators see: (a) Kilbinger, A. F. M.; Grubbs, R. H. *Angew. Chem., Int. Ed.* **2002**, *41*, 1563. (b) Borges, A. R.; Hyacinth, M.; Lum, M.; Dingle, C. M.; Hamilton, P. L.; Chruszcz, M.; Pu, L.; Sabat, M.; Caran., K. L. *Langmuir* **2008**, *24*, 7421. (c) Ryan, D. M.; Doran, T. M.; Nilsson, B. L. *Langmuir* **2011**, *27*, 11145.
(25) (a) Shriver-Lake, L. C.; Breslin, K. A.; Charles, P. T.; Conrad, D. W.; Golden, J. P.; Ligler, F. S. *Anal. Chem.* **1995**, *67*, 2431. (b) Shriver-Lake, L. C.; Donner, B. L.; Ligler, F. S. *Environ. Sci. Technol.* **1997**, *31*, 837. (c) van Bergen, S. K.; Bakaltcheva, I. B.; Lundgren, J. S.; Shriver-Lake, L. C. *Environ. Sci. Technol.* **2000**, *34*, 704.
(26) (a) Saxena, A.; Fujiki, M.; Rai, R.; Kwak, G. *Chem. Mater.* **2005**, *17*, 2181. (b) Yang, J.; Aschemeyer, S.; Martinez, H. P.; Trogler, W. C. *Chem. Commun.* **2010**, *46*, 6804. (c) He, G.; Yan, N.; Yang, J.; Wang, H.; Ding, L.; Yin, S.; Fang, Y. *Macromolecules* **2011**, *44*, 4759.
(27) (a) Brédas, J.-L.; Cornil, J.; Heeger, A. J. *Adv. Mater.* **1996**, *8*, 447. (b) Tan, C.; Atas, E.; Muller, J. G.; Pinto, M. R.; Kleiman, V. D.; Schanze, K. S. *J. Am. Chem. Soc.* **2004**, *126*, 13685.
(28) de Mello, J. C.; Wittmann, H. F.; Friend, R. H. *Adv. Mater.* **1997**, *9*, 230.